



Dissimilar micro beam welding of titanium to Nitinol and stainless steel using biocompatible filler materials for medical applications

Michael Wiegand¹ · Linda Marks² · Niklas Sommer¹ · Stefan Böhm¹

Received: 4 August 2022 / Accepted: 8 November 2022 / Published online: 16 November 2022
© The Author(s) 2022

Abstract

In the present investigation, thin sheet geometries of commercially pure titanium (cp, grade 4) are butt-welded to AISI 316L stainless steel as well as Nitinol by means of micro electron beam welding using filler materials. In order to avoid mixing of the base materials, the refractory metals tantalum, niobium and hafnium are applied as intermediate layers. Owing to the biocompatibility of these filler materials, the final products are suitable for medical technology applications. In combination with low energy inputs and precise beam alignments, it is demonstrated that high-quality and crack-free joints can be produced using micro electron beam welding. The welded joints are analysed using nanoindentation to identify critical weld areas, e.g. high concentrations of intermetallic compounds, and to evaluate the compatibility of the base and filler materials. To correlate the hardness mappings with the microstructural evolution of the welds, an exemplary joint is analysed by means of electron backscatter diffraction and energy dispersive X-ray spectroscopy with special emphasis on intermixing and the formation of intermetallic compounds. Based on the generated hardness mappings as well as the ultimate tensile strengths of the joints, it will be concluded which filler material provides the most promising results for the given material combinations.

Keywords Electron beam welding · Dissimilar welding · Filler material · Medical technology · Nanoindentation · Intermetallic compounds

1 Introduction and state-of-the-art

1.1 Dissimilar welding of metallic materials in medical technology

Titanium alloys, nickel-titanium shape memory alloys (NiTi) as well as stainless steels are commonly used materials in medical engineering. In addition to their excellent mechanical properties, these materials are particularly characterized by their exceptional corrosion resistance, thus making them indispensable in various medical technologies such as

implants and surgical instruments [1, 2]. Due to different material qualities and the need to optimize the functional, manufacturing and economic aspects of new and already existing products, it is desirable from both an industrial and a research point of view to produce dissimilar joints of titanium to NiTi and stainless steels, respectively. Figure 1 illustrates middle ear implants (stapes prostheses) as an example of a current application in the medical sector. The coupling element is made of NiTi, whereas the shaft is made of machined pure titanium, requiring a dissimilar connection at the junction.

While similar welding of the mentioned materials is generally possible, e.g. by means of beam welding processes, dissimilar fusion welding of titanium to stainless steel and NiTi is associated with various challenges. According to the Fe-Ti phase diagram, the joining of titanium to steel is limited by a low solubility of Fe in α -Ti (0.05–0.1% at room temperature) as well as the formation of the very brittle, ceramic-like intermetallic compounds (IMC) FeTi and Fe₂Ti [4, 5]. When using stainless steels with high content of chrome and nickel, other intermetallics such as TiCr₂, Ti₂Ni and Ti₃Fe₁₇Cr₅ may also be formed [5]. Fusion welding of

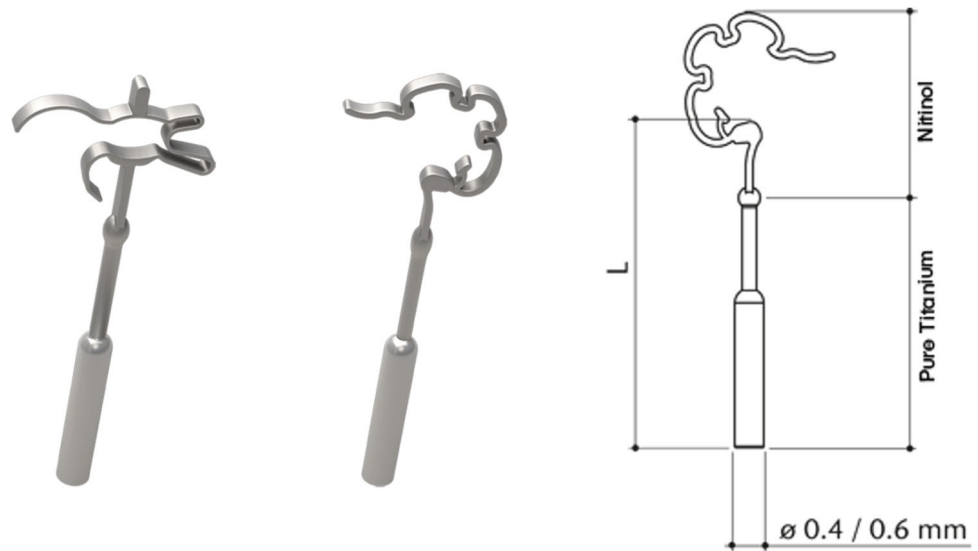
Recommended for publication by Commission IV - Power Beam Processes.

✉ Michael Wiegand
m.wiegand@uni-kassel.de

¹ Department for Cutting and Joining Manufacturing Processes, Institute for Production Technologies and Logistics, University of Kassel, Kurt-Wolters-Str. 3, Kassel, Germany

² NMI Natural and Medical Sciences Institute at the University of Tübingen, Markwiesenstr. 55, Reutlingen, Germany

Fig. 1 NiTiFLEX® and NiTi-BOND® stapes prostheses [3]



titanium to NiTi provides similar challenges. While NiTi itself is an intermetallic compound with exceptional mechanical properties, the required chemical composition between nickel and titanium is strictly limited [6]. Compositions deviating from this are, comparable to the joints with steel, associated with the formation of very brittle IMC (Ti_2Ni and Ni_3Ti) and, thus, provide low achievable strengths as well as high susceptibility to cracking [7]. Therefore, the use of more compatible filler materials as interlayers is considered to be expedient for both material combinations.

In addition, dissimilar fusion welded joints tend to have a high affinity for hot cracking. This can be attributed to deviating melting temperatures and the formation of eutectics, i.e. low-melting phases [8]. Therefore, dissimilar fusion welding requires precise control of the process parameters, their influence on heating and cooling rates as well as the position of the weld seam, making the beam welding processes highly suitable technologies for joining dissimilar welds [8]. Table 1 summarizes important characteristics of commercial pure (cp) titanium (grade 4), 316L (annealed) and Nitinol, which will be used as base materials in this investigation.

1.2 State-of-the-art in dissimilar beam welding of titanium to stainless steel

Titanium/stainless steel welded joints have been investigated in numerous studies over the past few years, as this specific material combination is not only of interest in medical technology but also in various other areas of application, e.g. the chemical and nuclear industries [5]. However, only poor mechanical properties and inconsistent reproducible welding results were achieved by autogenous welding as summarized below.

Shanmugarajan et al. [13] investigated laser welding of cp-Ti to 1.4301 stainless steel. Both pulsed and continuous-wave outputs failed to produce a durable joint. Satoh et al. [14] examined welding of cp-Ti to 316L and reported on achievable tensile strengths of up to 81.4 MPa using a pulsed laser source with different pulse durations as well as alternating beam offsets. However, the obtained strengths varied greatly, with a majority of the specimens failing immediately upon solidification. Chen et al. [15] were able to demonstrate that the positioning of the laser beam exerts a significant influence on the mechanical properties of the

Table 1 Selected properties of the alloys used in this investigation [9–12]. All properties given for a temperature of 20 °C

Base material	Melting point [°C]	Ultimate tensile strength [MPa]	Elongation at break [%]	Thermal conductivity [$Wm^{-1} K^{-1}$]	Coefficient of thermal expansion [$10^{-6} K^{-1}$]
cp-Titanium (grade 4)	1660	≥ 550	≥ 15	18	8.6
AISI 316L (X2CrNiMo17-12-2)	~ 1450	500–700 (annealed)	≥ 40 (annealed)	15	16
Nitinol (55.8 wt.-% Nickel)	1310	≥ 1070	≥ 10	18	11

titanium/stainless steel butt-welded joint. A maximum tensile strength of 150 MPa was achieved using a beam offset of 0.6 mm in the direction of the steel joining partner, thus limiting intermixing of titanium.

Electron beam welding of titanium to stainless steel has been investigated to a lesser extent compared to laser beam welding, although it offers various advantages [16]. The vacuum atmosphere provides optimal protection against environmental influences during the welding process, which is of great relevance when joining titanium due to its high affinity for volatile elements such as oxygen and nitrogen [17]. Furthermore, the process is known for its low heat input compared to other fusion welding processes. Therefore, melt pool sizes and, consequently, the areas of intermetallic compounds as well as their volume can be reduced significantly. In 2014, Wang et al. [12] tried joining Ti-6Al-2Zr-1Mo-1 V (TA 15) to 1.4301 stainless steel using electron beam welding. Again, without filler materials, no durable joint could be produced.

To prevent the intermixing of titanium and stainless steel and the formation of the very critical intermetallic compounds, many authors have used interlayers that exhibit enhanced chemical compatibility. However, research projects that investigated the use of filler materials mainly focused on materials that are not used in pure form in medical technology, such as copper [18–22], vanadium [21, 23, 24] and nickel [21]. Regardless of the filler materials selected, IMC still occur either on the titanium side or on the stainless steel side and, thus, constitute weak points. As a result, additional investigations were carried out in which multiple layers of filler materials were inserted and welded separately to further minimize chemical incompatibilities. Examples for tested material combinations are Nb/Cu [22, 23, 25], Nb/Ni [26] and Ta/Va/Fe [27]. Even though some of these combinations proved to create extremely durable welds, for example the Ta/Va/Fe-combination reached an UTS of up to 623 MPa with a fracture inside the unmolten vanadium, the use of exclusively biocompatible materials was not the prime focus of these investigations. Consequently, their use in medical technology is prohibited.

1.3 State-of-the-art in dissimilar beam welding of titanium to nickel-titanium

NiTi can show either superelasticity or the shape memory effect, depending on the exact composition of the material. Owing to its unique properties as well as good corrosion resistance, it finds a wide usage in medical applications like stents, implants or surgical tools like stone catch baskets [28]. However, its high price as well as poor machinability strengthens the need to create dissimilar material combinations with the much cheaper titanium. Yet, compared to

stainless steel, there are less investigations regarding the dissimilar fusion welding with titanium.

Shojaei Zoeram and Akbari Mousavi [29] as well as Miranda et al. [30] were unable to directly join Ti6Al4V to NiTi by laser welding due to direct failure of the weld metal resulted from the formation of intermetallic compounds. Again, using copper as an interlayer greatly increased the weldability, thus improving joint strengths up to 300 MPa [29]. In 2016, Oliveira et al. [31] used niobium as a diffusion barrier for the identical material combination and were able to achieve similar tensile strengths. Ge et al. [32] investigated niobium in overlapping configuration between Nitinol and Ti2AlNb, proving it is possible to create sound joints with intermixing the filler material into the weld. Once again, even though there are studies that exclusively used biocompatible filler materials, the results reveal the need and the potential to further optimize the fusion process of these combinations in order to create reproducible high-quality and durable welds.

1.4 Scope of the present investigation

The present study thus details the use of micro electron beam welding to produce high-quality and durable joints between titanium and stainless steel as well as nickel-titanium alloys by using *biocompatible* filler materials. For this purpose, the welding parameters are selected to minimize the energy input and weld pool size while ensuring a sufficient welding depth and fusion with each of the high-melting filler materials. As the proportion of molten filler material and intermixing with either 316L or NiTi have a decisive influence on the microstructural and mechanical properties, a beam offset in the direction of the base materials is partly implemented in order to affect the weld composition and thereby prevent hot cracks as well as spontaneous fractures. The samples are characterized using optical light microscopy as well as nanoindentation. It will be demonstrated that nanoindentation is a qualified tool to identify critical areas of the weld seams and to precisely deduce the resulting weak points of the joints. In combination with electron backscatter diffraction analyses and tensile tests, the present investigation will reveal the most promising filler materials for both material combinations and, thus, substantially enlarges the known state-of-the-art.

2 Materials and methods

Thin sheet geometries with the dimension 12.5 mm × 25 mm × 0.25 mm, made of titanium grade 4, 316L (annealed) and Nitinol were produced by electrical discharge machining (EDM) and used as welding specimens.

Table 2 Chemical composition of titanium grade 4 (a), Nitinol (b) and 316L (c) as specified by the material suppliers

(a) Element (wt.-%) — titanium grade 4									
Ti	C	N	Fe	O					
Bal	0.011	0.010	0.12	0.31					
(b) Element (wt.-%) — Nitinol									
Ni	Ti	C	O	Fe	Other single trace elements				
55.94	Bal	0.0275	0.019	0.014	<0.01				
(c) Element (wt.-%) — 316L									
Fe	C	Si	Mn	P	S	Cr	Ni	Mo	
Bal	Max. 0.03	Max. 1.0	Max. 2.0	Max. 0.045	Max. 0.03	16.5–18.5	10.0–13.0	2.0–2.5	

Table 3 Overview of welding parameters

Accelerating voltage [kV]	Beam current [mA]	Welding speed [mm/s]	Focus position	Beam offset (on titanium) [mm]	Beam offset (on 316L/NiTi) [mm]
60	1.35, continuous	40	surface	0.1 (Ta) 0.075 (Nb & Hf)	0 (Ta) 0.075 (Nb & Hf)

The chemical composition of the sheets is depicted in Table 2.

The filler materials were identically manufactured into thin strips measuring approximately 12.5 mm × 0.25 mm × 0.25 mm. The eroded joining edges of the samples were carefully ground with fine silicone-carbide paper to remove the process-related oxidation layers. Subsequently, the samples were cleaned using acetone and dried in air. To ensure a precise, virtually gap-free positioning for butt welding, the specimens were clamped individually in a special fixture that also allowed welding of two samples during one evacuation. The filler material was held in position by applying light pressure through lateral clamping jaws.

As beam source, a micro electron beam welding machine (SEM108, pro-beam GmbH & Co. KGaA, Gilching, Germany as well as JSC Selmi, Sumy, Ukraine) was used for the experiments. The welding machine was equipped with a beam generator that allows beam currents of up to 20 mA at an acceleration voltage of 60 kV. An oil-free turbo pump vacuum system provides vacuum atmospheres as low as 10⁻⁶ mbar for an optimal protection of the weld seam.

Furthermore, beam diameters of approximately 30 μm can be achieved at 1 mA beam current.

The welding parameters used for the presented samples are displayed in Table 3. In order to affect the amount of molten filler metal, prevent mixing of the base materials and ultimately to produce crack-free joints, different beam offsets on the base materials were applied. A more detailed explanation of the necessity of using the beam offsets is provided in “Sect. 3.1.” Fig. 2 visualizes the welding configuration in schematic form.

Table 4 shows important properties of the filler materials used in this investigation. The refractory metals niobium, tantalum and hafnium were selected for this study based on their natural biocompatibility and their ability to form solid solutions with titanium.

The weld seams were inspected with the aid of optical light microscopy (DM2700, Leica Microsystems GmbH, Wetzlar, Germany). For this purpose, the welded specimens were ground to the centre of the weld using silicone-carbide paper and subsequently polished using a diamond suspension (grit size 0.1 μm). The etchants used were V2A-etchant (60 s at 60 °C) to highlight the steel structure and an etching solution according to Keller (120 s at room temperature) to highlight the titanium structure. A subsequent, detailed analysis of the weld between tantalum and 316L is carried out by means of scanning electron microscopy (SEM, Zeiss REM Ultra Plus, Carl Zeiss AG, Oberkochen) at an acceleration voltage of 20 kV. For this purpose, the corresponding sample was polished again using a 0.25 μm colloidal Si-suspension. With the help of energy dispersive X-ray spectroscopy (EDS, Bruker XFlash 6160, Bruker Corporation, MA, USA), as well as electron backscatter diffraction

Fig. 2 Schematic illustration of the welding process

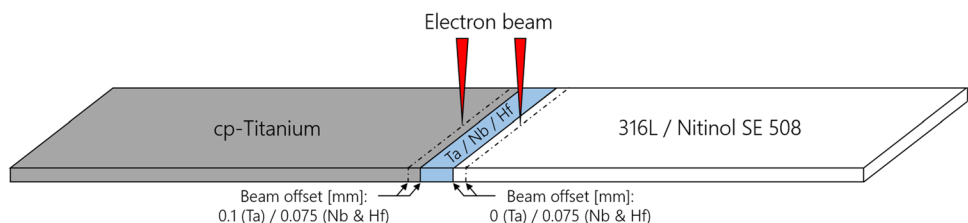


Table 4 Selected properties of the refractory metals used in this investigation [33, 34]. Mechanical properties (*) are based on internal tension tests using the provided material. Purity values as provided by material supplier. All properties given for a temperature of 20 °C

Filler material	Melting point [°C]	Ultimate tensile strength [MPa]	Elongation at break [%]	Thermal conductivity [$\text{Wm}^{-1} \text{K}^{-1}$]	Coefficient of thermal expansion [10^{-6}K^{-1}]
Niobium 99.9%	2468	~470*	~5*	52	7.1
Tantalum 99.9%	2996	~370*	~32*	54	6.5
Hafnium 99+ %	2233	~402*	~23*	23	5.9

(EBSD, Bruker e⁻-flash, Bruker Corporation, MA, USA), detailed statements about the phase formation as well as the microstructural evolution can be provided.

Tensile tests were carried out on basis of DIN EN ISO 6892–1 on a universal testing machine (Z100, ZwickRoell AG, Ulm, Germany). The specimens were clamped using a slight preload of 5 N and subsequently tested with regard to their ultimate tensile strength and elongation at break. The tensile testing samples, whose geometry is illustrated in Fig. 3, were extracted using EDM. The mechanical properties were determined using three identically manufactured specimens for each parameter and material combination.

Microhardness measurements were conducted using a nanoindentation tester (NHT², Anton Paar GmbH, Graz, Austria) at a maximum load of 10 mN with a loading and unloading speed of 100 mN/s. In order to fulfill the high requirements of a plane surface finish, the specimens were prepared in multiple short grinding and polishing steps. The preparation was completed with a final polish using a 0.25 μm colloidal Si-suspension mixed with a 30% hydrogen peroxide solution (ratio 9:1).

3 Results and discussion

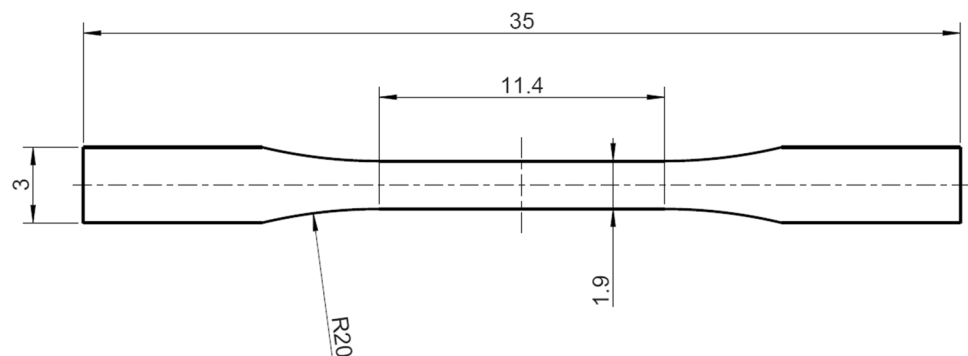
3.1 General observations

An inspection of the weld bead surface following the welding experiments as well as microscopic analyses reveal that all investigated material combinations can be welded

without cracks using micro electron beam welding with optimized process parameters. The refractory metals niobium, tantalum and hafnium are known to form intermetallic compounds with Fe as well as Ni [35, 36]. The present study shows that these intermetallics appear to be less critical than the reported brittle phases between Fe-Ti and Ti-Ni and that their formation range can be reduced through the use of optimized process parameters. An examination of individual joints in the following paragraphs confirms that the proportion of molten filler material is particularly decisive for the properties of the weld seams between the refractory metals and 316L as well as Nitinol. As a result, some material combinations are characterized by the formation of small transverse cracks or even complete failure immediately during the welding process once no beam offset is applied and, consequently, more filler material is mixed into the weld, as can be seen in Fig. 4a and b.

In order to reduce the proportion of filler material in the weld and to produce crack-free specimens, a beam offset of 0.075 mm to 316L/NiTi was applied for the samples welded with both niobium and hafnium. For the specimens welded with tantalum as filler metal, no beam offset is necessary to generate crack-free weld seams with 316L as well as NiTi. This can be attributed to the lower amount of molten and intermixed filler material and will be explained in more detail in the following section.

Besides the general chemical compatibilities, the thermo-physical properties of the filler materials differ greatly from those of both base materials. Nevertheless, by applying the aforementioned parameter sets (cf. Table 3), the welding

Fig. 3 Sample geometry employed for tensile testing

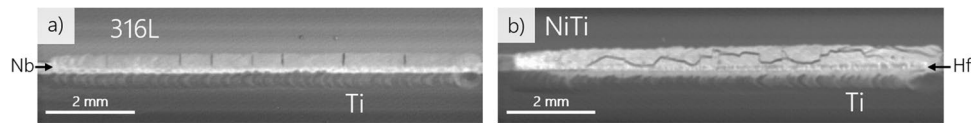


Fig. 4 Weld seam surface of samples welded with niobium (a) and hafnium (b) using no beam offset. The electron-optical images were captured by the electron beam welder using backscattered electrons

tests did not reveal any further welding problems, such as hot cracks. This leads to the conclusion that even strongly differing material properties can be counteracted using micro electron beam welding in combination with high welding speeds as well as precise beam positioning.

As expected, based on the good compatibility between titanium and the investigated filler metals, the associated welds on the titanium side were crack-free and none of the tensile specimens failed therein. As a result, only weld seams between the refractory metals and 316L as well as NiTi shall be considered in further detail in the following sections.

Furthermore, internal preliminary welding tests showed that mixing of the base materials should be strictly avoided. Specimens in which such mixing occurs are characterized by poor mechanical properties, as the resulting brittle IMC promote premature failure in tensile tests. To increase the distance between the weld seams and consequently prevent contact of the base materials, a beam offset of 0.075 mm (Nb and Hf) and 0.1 mm (Ta) is applied on the titanium side (cf. Table 3).

3.2 Cp-titanium/316L stainless steel

Using tantalum as an interlayer between titanium and 316L, all welding tests are characterized by excellent weldability, resulting in defect-free specimen. Although no beam offset is used on the stainless steel side of the sample presented below, the amount of molten tantalum is relatively low as can be seen by the sharp interface at the transition to the weld in Fig. 5a. This is due to the fact that tantalum has a comparatively high-melting temperature as well as thermal conductivity rate (cf. Table 4). However, considering the corresponding hardness mapping in Fig. 5b, the weld seam between tantalum and 316L is characterized by high hardness values compared to the base materials, averaging at approximately 600 HV. This confirms a mixing of the tantalum material into the weld and hints the formation of intermetallic compounds. Moreover, a small area of high hardness values above 800 HV can be identified. In this region, the proportion of molten tantalum appears to be higher as can be seen in the cross section of the joint.

To further quantify the findings of the hardness mappings, this material combination is examined in detail using SEM. Figure 5c illustrates a combined inverse pole figure mapping (IPFM) and superimposed image quality mapping

(IQM) of the transition zone between the unmolten tantalum and the weld seam. Starting from the fusion line, numerous grains with strongly alternating size and orientation can be observed in a range of approximately 40 μm within the weld. Despite the different morphologies, this area appears to consist almost entirely of face-centred cubic (fcc) austenite, as shown by the phase mapping (PM) in Fig. 5d. In addition to that, the PM reveals the existence of the intermetallic compounds FeTa and Fe₂Ta. These intermetallics are particularly concentrated along the fusion line and measure about 3 μm in width. Moreover, it can be observed that smaller volumes of the IMC exist outside the transition zone and accumulate especially at grain boundaries. A correlation between the determined phases and the weld composition can be obtained by EDS analysis. As can be derived from Fig. 5e, the transition area between tantalum and the weld, where large intermetallics are present, contains high proportions of tantalum which decrease in the direction of the 316L stainless steel. Nevertheless, a significant amount of tantalum can still be detected outside of the IMC cluster. The determined mass fraction inside the weld is comparable to the proportion of chromium and, thus, explains the detected fine distribution of intermetallic compounds as well as the high hardness values across the weld seam.

As mentioned before, with the use of niobium and hafnium as interlayers between titanium and 316L, a beam displacement of at least 0.075 mm to 316L is necessary to produce crack-free specimens. In comparison to tantalum, the amount of molten filler metal is significantly higher despite the beam offset, as can be seen by the uneven transition between the filler materials and the weld seams in Fig. 6a and b. This can be attributed to the lower melting point and thermal conductivity of niobium and hafnium compared to tantalum (cf. Table 4). In both cross sections, narrow areas with a different morphologic structure are visible along the fusion line between tantalum and the steel-sided weld seam. As confirmed by the hardness mappings, these areas consist of compositions that result in extremely high hardness values of up to 1300 HV, again proving that high contents of the refractory metals support the formation of IMC. The hardness values in the remaining part of the weld seam are significantly lower, averaging at approximately 650 HV and 600 HV for Nb and Hf, respectively. Based on the hardness mapping as well as the SEM analysis of the previous sample with tantalum, similar mixing

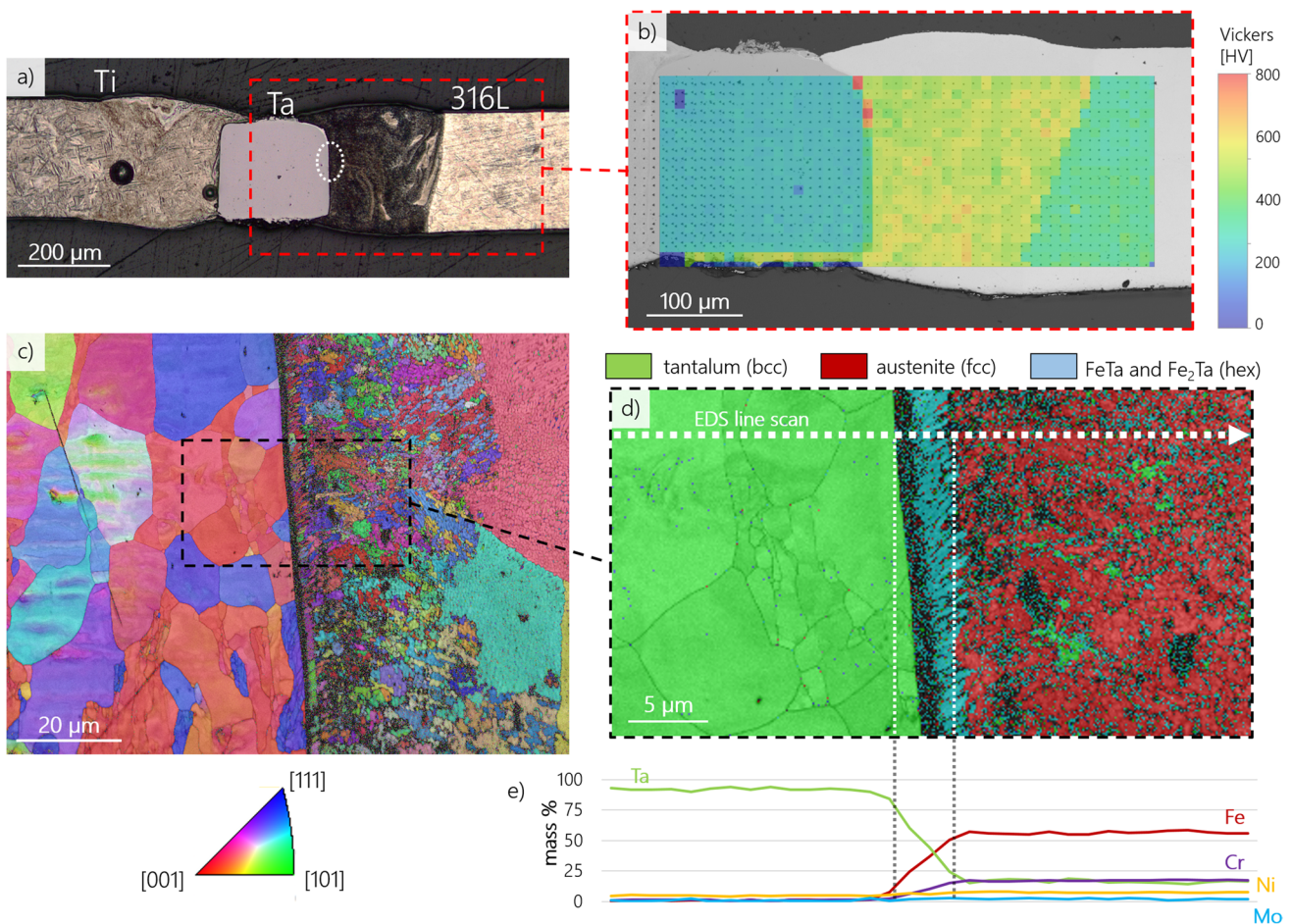


Fig. 5 **a** Cross section of the titanium/stainless steel sample with tantalum as interlayer using no beam offset on stainless steel and 0.1 mm offset on titanium. The red rectangle represents the area of interest for corresponding nanoindentation analysis in **b**. The blue rectangle

marks the area analysed by EBSD: **c** combined IQM and IPFM of the fusion line between tantalum and the weld. Grain orientations plotted parallel to the cross section. **d** Combined IQM and PM of the transition zone. **e** Results of the EDS line scan in the transition zone

conditions in the weld can be assumed. Thus, a fine distribution of intermetallics is most likely to exist inside the weld seam, which explains the increased hardness values in comparison to the base materials.

Further correlations between mechanical properties, microstructural evolution and failure mode can be derived from the tensile tests. As illustrated in Fig. 7a, the transition between the filler metal and the steel-sided weld act as weak points with every joint failing in these regions. However, the values of ultimate tensile strength and elongation at break vary greatly for the different filler materials used, as shown in Fig. 7b. The welded samples with hafnium, which show a very wide range with high concentrations of intermetallic compounds based on the hardness mapping, are characterized by comparatively low and strongly fluctuating UTS values. With respect to the nanoindentation carried out, this confirms that the identified areas containing a comparatively high proportion of intermetallics have a decisive influence on the mechanical properties of the titanium/

stainless steel joints and should be minimized. Significantly better strength values are achieved with both niobium and tantalum as filler materials. In particular, ultimate tensile strengths with only minor variation between the samples can be achieved through the use of Ta. Moreover, the average UTS of 374 MPa corresponds closely to the mechanical properties of the Ta material used (cf. Table 4).

As a result of the analyses presented beforehand, the formation of intermetallic compounds can be confirmed for every filler metal and 316L. Ultimately, the proportion of the molten filler material determines the dimension of critical phase ranges and should therefore be minimized. In this investigation, the latter was achieved by the use of a beam offset to the base materials in combination with high welding speeds and small weld pools. The sample with tantalum as filler material shows the best results in this regard, which, in addition to parameter optimization, is attributed to the high-melting temperature and thermal conductivity yielding a low proportion and a very narrow range with high

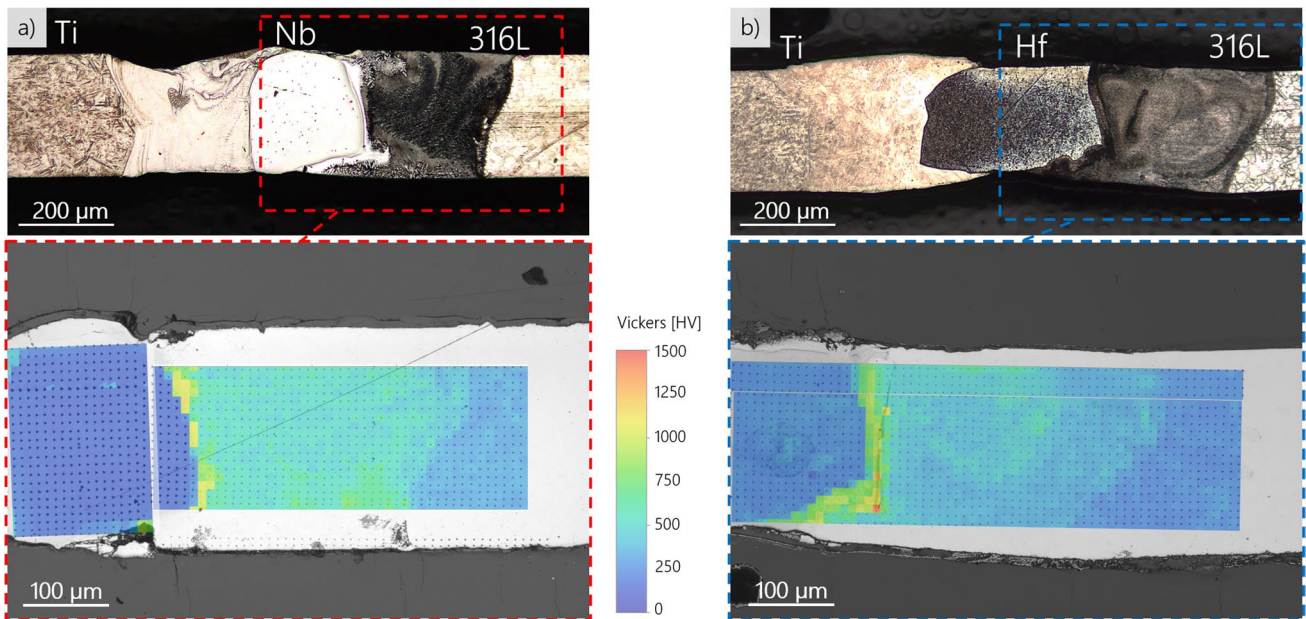


Fig. 6 Cross section of the titanium/stainless steel joints using niobium (a) and hafnium (b) as interlayers, both welded with a beam offset of 0.075 mm on the base materials. The coloured rectangles represent areas of interest for the corresponding nanoindentation analysis

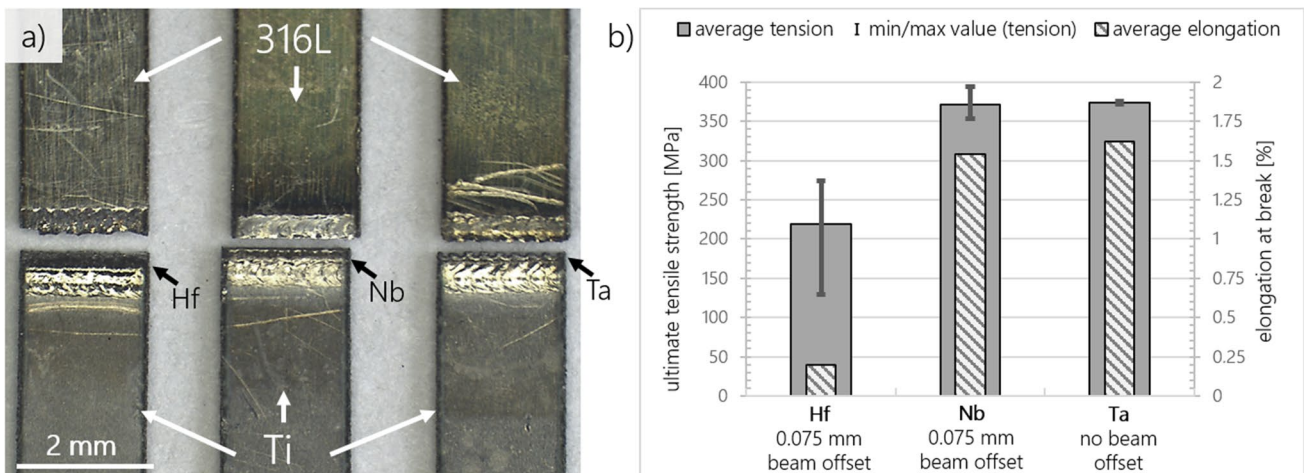


Fig. 7 a Macroscopic images of exemplary specimens after the tensile tests. b Summary of obtained mechanical properties for each filler material used for the titanium/stainless steel welded joints

concentrations of IMC. In combination with the excellent results of the tensile tests, it is evident that the most promising results in the course of this investigation were obtained by using tantalum as a filler material for the titanium/stainless steel joints.

3.3 Cp-titanium/Nitinol

All welding tests of the material combination titanium/NiTi carried out within the scope of this investigation show excellent weldability when using either niobium or tantalum as

intermediate layers. Regardless of the beam offset, all associated weld specimens are crack-free. In order to relate the results from the analyses to the results of titanium/stainless steel joints presented beforehand, samples using identical beam offsets are considered in detail below.

Based on the microstructural examinations of the joints in Fig. 8a and b, no distinctive etching reactions or microstructural changes can be detected on the fusion line between the filler materials and Nitinol. The corresponding hardness mappings confirm the apparently very good compatibility of Nitinol with the filler materials tantalum and niobium. No

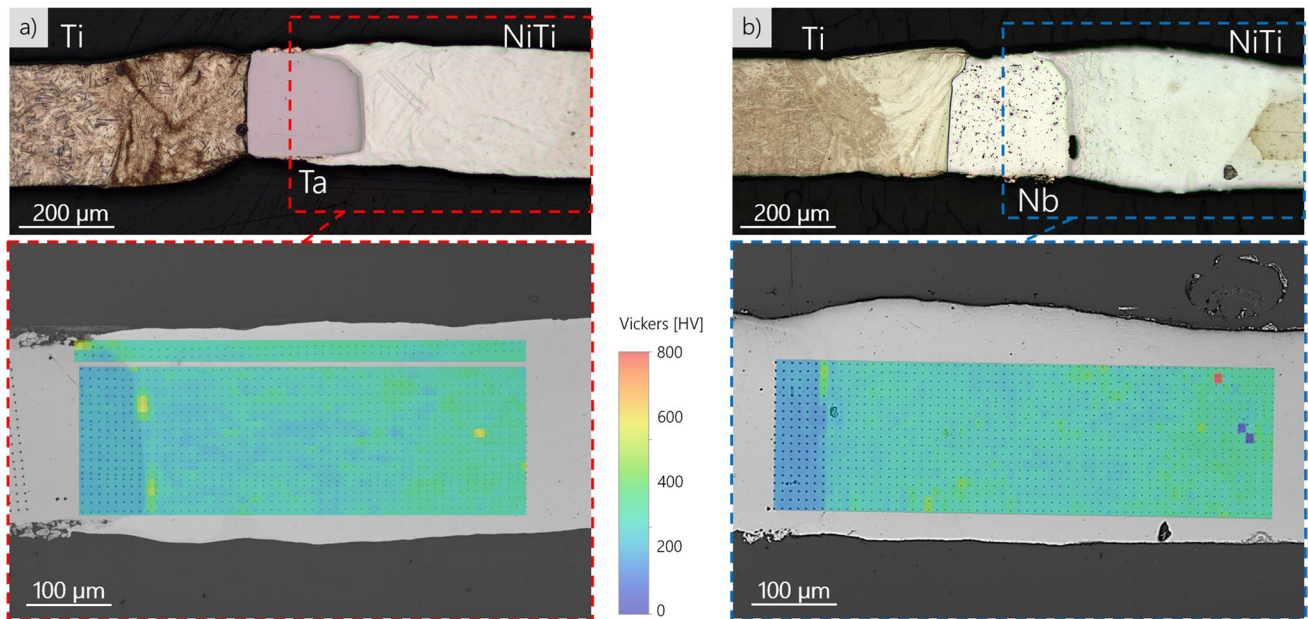


Fig. 8 Cross section of the titanium/NiTi joints with tantalum (a) as interlayer using no beam offset on NiTi and 0.1 mm offset on titanium and with niobium (b) as interlayer using 0.075 mm beam offset on

both base materials. The coloured rectangles represent areas of interest for the corresponding nanoindentation analysis

segregations with high proportions of IMC can be identified using nanoindentation. This needs to be particularly emphasized for the transition region where higher proportions of the filler materials are to be expected. The joints presented mostly feature relatively low hardness values with an average of approximately 380 HV. Only individual values are noticeably higher for the joint with tantalum. As mentioned previously, both tantalum and niobium form IMC with nickel and are most likely to mix into the weld in a non-negligible proportion, as can be concluded by the EDS line scan in the preceding section. This leads to the assumption that the comparatively low proportion of nickel material (55.94 wt.-%) and the good compatibility of the filler materials with the titanium proportion lead to non-critical compositions within the weld seams.

In contrast to the excellent welding results with niobium and tantalum, the welding tests with hafnium as an interlayer immediately fractured within the Nitinol seam during the welding process using no beam offset (cf. Figure 4b). However, by applying a beam offset of 0.075 mm to the NiTi base material, crack-free welds can be produced in a reproducible manner. The corresponding cross section of the joint in Fig. 9 shows a strongly pronounced etching reaction along the transition between hafnium and NiTi, as highlighted by the white dots. As confirmed by the nanoindentation mapping, this area contains a distinct concentration of IMC with high hardness peaks. From this observation, it can be deduced that, compared to niobium and tantalum, hafnium is more prone to the formation of

critical intermetallic compounds with Nitinol and therefore features the poorest compatibility.

The results obtained from the hardness analyses show clear correlations to the tensile tests carried out. As expected, all tensile specimens welded with hafnium fail in the transition between Hf and the NiTi-sided weld due to the high hardness peaks, as exemplified in Fig. 10a. In contrast, both dissimilar joints with niobium and tantalum fracture within the unmolten filler metal. The average UTS values of 453 MPa and 370 MPa for Nb and Ta, respectively, correspond very well to the initial mechanical properties of the fillers. Small variations are most likely due to slight irregularities in the properties of the foil material. The tensile tests therefore confirm the good compatibility with both, titanium and Nitinol. Finally, the best strength and elongation values are obtained using niobium, which in turn can be attributed to the higher strength of niobium compared to tantalum.

Based on the detailed analyses and the subsequent tensile tests, it can be confirmed that the nanoindentation has a high informative value regarding the mixing of the weld metals as well as the existence of IMC in dissimilar welding. Only extremely narrow concentration ranges, such as the titanium/316L sample with tantalum as an intermediate layer, require high-resolution EBSD analysis. Nevertheless, the microhardness mappings determined serve excellently to identify critical weld seam areas, which ultimately have a decisive influence on the mechanical properties of the joint.

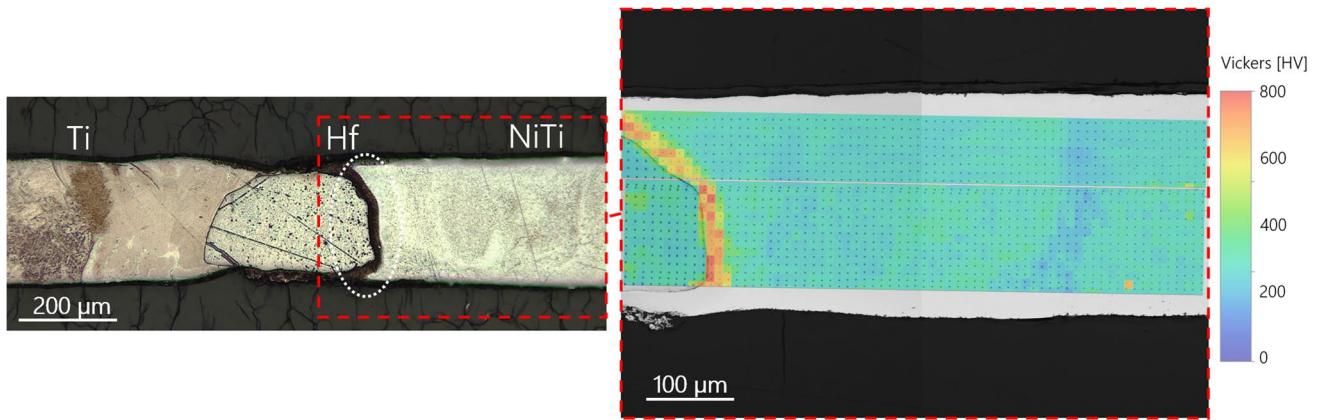


Fig. 9 Cross section of the titanium/NiTi joint with hafnium as interlayer using 0.075 mm beam offset on both base materials. The red rectangle represents the area of interest for corresponding nanoindentation analysis

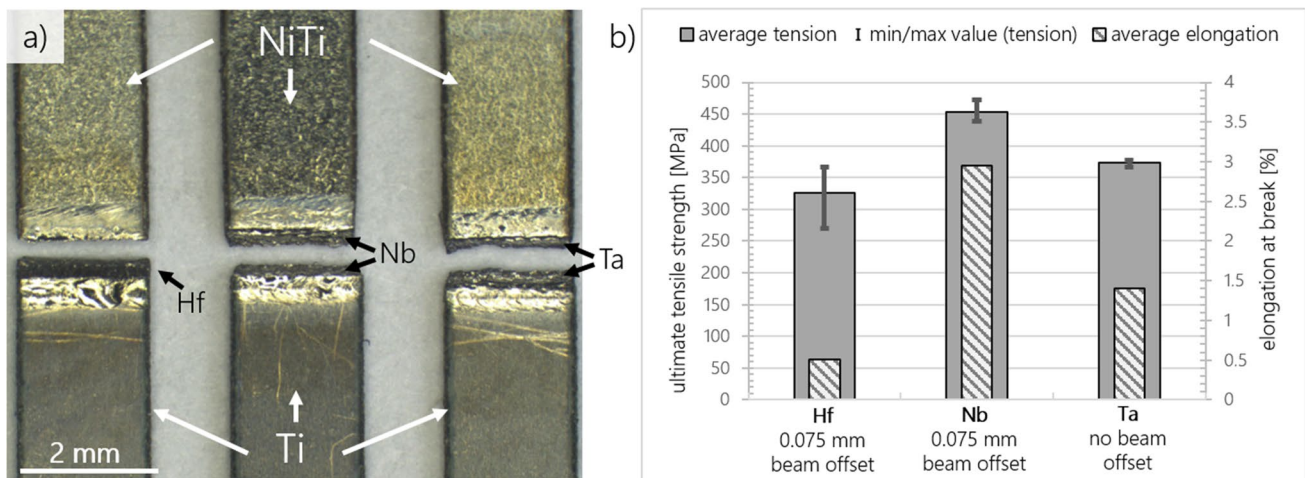


Fig. 10 a Macroscopic images of exemplary specimens after the tensile tests. b Summary of obtained mechanical properties for each filler material used for the titanium/NiTi welded joints

4 Conclusion

In the investigation at hand, thin sheets of pure titanium were electron beam welded to 316L stainless steel as well as Nitinol in butt-joint configuration with the aid of the biocompatible filler materials niobium, tantalum and hafnium as interlayers. Based on the results presented beforehand, the following conclusions can be drawn:

- By optimizing the parameters with regard to low energy inputs in combination with precise beam alignments, it is possible to produce defect-free welds for all material combinations investigated using micro electron beam welding.
- The chemical composition and particularly the amount of molten and intermixed filler material is found to

have a major influence on the weldability, the formation of intermetallic compounds and finally the mechanical properties of the joint. For some material combinations, a beam offset in the direction of the base materials is necessary to reduce the proportion of the filler material in the weld and consequently the areas with critical hardness concentrations.

- Tantalum proves to be the most promising filler material for the titanium/stainless steel joint as the highest average UTS is obtained, which also matches the mechanical properties of the tantalum material used in this study.
- For the titanium/Nitinol combination, both joints welded with niobium and tantalum are characterized by both excellent weldability and mechanical properties under quasi-static stress. Nanoindentation proved the good compatibility of the filler materials to Nitinol, as no criti-

cal hardness peaks are found. For both joints, the tensile specimens fail inside the filler metal.

- When applying a filler material between titanium and stainless steel or NiTi, a mixing of the base materials should be avoided as the resulting brittle IMC compositions result in drastic weak points.

Acknowledgements The corresponding author thankfully acknowledges the support provided within the framework of “DVS IiW Young Professionals” by the German Welding Society. Furthermore, the authors would like to express their gratitude to Heinz Kurz GmbH (Dußlingen, Germany) for providing sheet materials used in the present study. In addition to that, the authors would like to thank the technician employees and student assistants for their continuous support.

Author contribution M.W.: conceptualization, writing, project administration, execution of welding tests, data evaluation.

L.M.: review and editing, execution of the nanoindentation mappings.

N.S.: review and editing, execution of the EBSD analyses.

S.B.: review and editing, supervision, funding acquisition.

Funding Open Access funding enabled and organized by Projekt DEAL. The shown results were achieved in the project “Artfremdes Mikro-Strahlschweißen von Titan mit Nitinol und nichtrostenden Stählen zur Herstellung eines biokompatiblen Materialverbunds unter Verwendung von Zusatzwerkstoffen (MeTiWeld)” (reference IGF 21.601 N), which is supervised by the Forschungsvereinigung Schweißen und verwandte Verfahren e.V. of the German Welding Society and funded by the German Federation of Industrial Research Associations (AiF) by means of the Federal Ministry for Economic Affairs and Climate Action (BMWK) on the basis of a decision by the German Bundestag.

Data availability Data of the present publication cannot be disclosed as they are part of an ongoing investigation.

Declarations

Conflict of interest The authors declare no competing interests.

Open Access This article is licensed under a Creative Commons Attribution 4.0 International License, which permits use, sharing, adaptation, distribution and reproduction in any medium or format, as long as you give appropriate credit to the original author(s) and the source, provide a link to the Creative Commons licence, and indicate if changes were made. The images or other third party material in this article are included in the article's Creative Commons licence, unless indicated otherwise in a credit line to the material. If material is not included in the article's Creative Commons licence and your intended use is not permitted by statutory regulation or exceeds the permitted use, you will need to obtain permission directly from the copyright holder. To view a copy of this licence, visit <http://creativecommons.org/licenses/by/4.0/>.

References

- Fazel-Rezai R (ed) (2011) Biomedical engineering, from theory to applications. London, United Kingdom, IntechOpen [Online]. Available from: <https://www.intechopen.com/books/2241>, <https://doi.org/10.5772/2629>
- Petrini L, Migliavacca F (2011) Biomedical applications of shape memory alloys. *J Metall* 2011:1–15. <https://doi.org/10.1155/2011/501483>
- NiTiFLEX® and NiTiBOND® stapes prostheses — with friendly permission by Heinz-Kurz-GmbH, Dußlingen, www.kurzmed.com. More information on the prostheses can be found in the official product catalogue, available at <https://www.kurzmed.com/de/bibliothek.html>. Accessed 15 Nov 2022
- Cacciamani G, de Keyzer J, Ferro R, Klotz UE, Lacaze J, Wollants P (2006) Critical evaluation of the Fe–Ni, Fe–Ti and Fe–Ni–Ti alloy systems. *Intermetallics* 14(10–11):1312–1325. <https://doi.org/10.1016/j.intermet.2005.11.028>
- Quazi MM, Ishak M, Fazal MA, Arslan A, Rubaiee Saeed, Abdullah Qaban MH, Aiman Tipu Sultan, Ali MM, Manladan SM (2020) Current research and development status of dissimilar materials laser welding of titanium and its alloys. *Opt Laser Technol* 126:106090. <https://doi.org/10.1016/j.optlastec.2020.106090>
- Massalski TB, Okamoto H, Subramanian PR, Kacprzak L (eds) (1990) Binary alloy phase diagrams, vol 3. ASM International, Metals Park, Ohio
- Hu L, Xue Y, Shi F (2017) Intermetallic formation and mechanical properties of Ni-Ti diffusion couples. *Mater Des* 130:175–182. <https://doi.org/10.1016/j.matdes.2017.05.055>
- Schuster J (2004) Heißrisse in Schweißverbindungen - Entstehung, Nachweis und Vermeidung. Düsseldorf, Verlag für Schweißen und Verwandte Verfahren DVS-Verlag
- METALCOR GmbH (2022) “Datenblatt: Titan-Grade 4 (3.7065)”. <http://www.metalcor.de/datenblatt/124/>. Accessed 22 Jul 2022
- Deutsche Edelstahlwerke GmbH (2016) “Werkstoffdatenblatt 1.4404”. https://www.dew-stahl.com/fileadmin/files/dew-stahl.com/documents/Publikationen/Werkstoffdatenblaetter/RSH/1.4404_de.pdf. Accessed 22 Jul 2022
- NDC® Nitinol Materials, Manufacturing, and Technical Services by Confluent Medical Technologies (2022) “Superelastic nitinol alloys — material data sheet”. <https://confluentmedical.com/wp-content/uploads/2016/01/Material-Data-Sheet-Superelastic.pdf>. Accessed 22 Jul 2022
- Hellberg S, Hummel J, Krooß P, Niendorf T, Böhm S (2020) Microstructural and mechanical properties of dissimilar Nitinol and stainless steel wire joints produced by micro electron beam welding without filler material. *Weld World* 64(12):2159–2168. <https://doi.org/10.1007/s40194-020-00991-3>
- Shanmugarajan B, Padmanabham G (2012) Fusion welding studies using laser on Ti–SS dissimilar combination. *Opt Lasers Eng* 50(11):1621–1627. <https://doi.org/10.1016/j.optlaseng.2012.05.008>
- Satoh G, Yao YL, Qiu C (2013) Strength and microstructure of laser fusion-welded Ti–SS dissimilar material pair. *Int J Adv Manuf Technol* 66(1–4):469–479. <https://doi.org/10.1007/s00170-012-4342-6>
- Chen S, Zhang M, Huang J, Cui C, Zhang H, Zhao X (2014) Microstructures and mechanical property of laser butt welding of titanium alloy to stainless steel. *Mater Des* 53:504–511. <https://doi.org/10.1016/j.matdes.2013.07.044>
- Sun Z, Karppi R (1996) The application of electron beam welding for the joining of dissimilar metals: an overview. *J Mater Process Technol* 59(3):257–267. [https://doi.org/10.1016/0924-0136\(95\)02150-7](https://doi.org/10.1016/0924-0136(95)02150-7)
- Lütjering G, Williams JC (2007) Titanium, 2nd edn. Springer, Berlin, New York
- Kumar R, Balasubramanian M (2020) Analysis and comparison of diffusion bonded and friction welded Ti-6Al-4V and stainless steel joints with copper as interlayer. *MaterToday: Proc* 21:1467–1473. <https://doi.org/10.1016/j.matpr.2019.11.047>
- Zhang Y, Sun DQ, Gu XY, Liu YJ (2017) Nd/YAG pulsed laser welding of TC4 titanium alloy to 301L stainless steel via pure

- copper interlayer. *Int J Adv Manuf Technol* 90(1–4):953–961. <https://doi.org/10.1007/s00170-016-9453-z>
20. Zhang Y, Chen Y, Zhou J, Sun D, Gu X (2020) Forming mechanism and mechanical property of pulsed laser welded Ti alloy and stainless steel joint using copper as interlayer. *J Market Res* 9(2):1425–1433. <https://doi.org/10.1016/j.jmrt.2019.11.068>
 21. Wang T, Zhang B, Feng J (2014) Influences of different filler metals on electron beam welding of titanium alloy to stainless steel. *Transac Nonferrous Metals Soc China* 24(1):108–114. [https://doi.org/10.1016/S1003-6326\(14\)63034-X](https://doi.org/10.1016/S1003-6326(14)63034-X)
 22. Li J, Liu Y, Gao Y, Jin P, Sun Q, Feng J (2020) Benefits of interfacial regulation with interlayers in laser welding Ti6Al4V/316L steel. *Opt Laser Technol* 125:106007. <https://doi.org/10.1016/j.optlastec.2019.106007>
 23. Mannucci A, Tomashchuk I, Mathieu A, Bolot R, Cicala E, Lafaye S, Roudeix C (2020) Use of pure vanadium and niobium/copper inserts for laser welding of titanium to stainless steel. *J Adv Join Proc* 1:100022. <https://doi.org/10.1016/j.jajp.2020.100022>
 24. Zhang Y, Zhou J, Sun D, Li H (2020) Two pass laser welding of TC4 titanium alloy to 301L stainless steel via pure V interlayer. *J Market Res* 9(2):1400–1404. <https://doi.org/10.1016/j.jmrt.2019.11.066>
 25. Fang Y, Jiang X, Song T, Mo D, Luo Z (2019) Pulsed laser welding of Ti-6Al-4V titanium alloy to AISI 316L stainless steel using Cu/Nb bilayer. *Mater Lett* 244:163–166. <https://doi.org/10.1016/j.matlet.2019.02.075>
 26. Zhang Y, Zhou J, Sun D, Li H (2020) Three-pass laser welding of Ti alloy-stainless steel using Nb and Ni interlayers. *J Market Res* 9(2):1780–1784. <https://doi.org/10.1016/j.jmrt.2019.12.009>
 27. Zhang Y, Sun DQ, Gu XY, Duan ZZ, Li HM (2018) Nd:YAG pulsed laser welding of TC4 Ti alloy to 301L stainless steel using Ta/V/Fe composite interlayer. *Mater Lett* 212:54–57. <https://doi.org/10.1016/j.matlet.2017.10.057>
 28. Nasakina EO, Sevostyanov MA, Baikin AS, Seryogin AV, Konushkin SV, Sergienko KV, Leonov AV, Kolmakov AG (2017) Applications of nanostructural NiTi alloys for medical devices. In: Ebrahim F (ed) *Shape Memory Alloys - Fundamentals and Applications*. <https://doi.org/10.5772/intechopen.69238>
 29. ShojaeiZoeram A, Akbari Mousavi S (2014) Laser welding of Ti-6Al-4V to Nitinol. *Mater Design* 61:185–190. <https://doi.org/10.1016/j.matdes.2014.04.078>
 30. Miranda RM, Assunção E, Silva RJC, Oliveira JP, Quintino L (2015) Fiber laser welding of NiTi to Ti-6Al-4V. *Int J Adv Manuf Technol* 81(9–12):1533–1538. <https://doi.org/10.1007/s00170-015-7307-8>
 31. Oliveira JP, Panton B, Zeng Z, Andrei CM, Zhou Y, Miranda RM, BrazFernandes FM (2016) Laser joining of NiTi to Ti6Al4V using a Niobium interlayer. *Acta Mater* 105:9–15. <https://doi.org/10.1016/j.actamat.2015.12.021>
 32. Ge F, Oliviera JP, Ke W, Teshome FB, Li Y, Zeng Z (2021) Dissimilar laser welding of a NiTi shape memory alloy to Ti2AlNb. *Metals* 11(10):1578. <https://doi.org/10.3390/met11101578>
 33. Nagler Normalien GmbH, “NE-Metalle”. https://normalien.de/media/pdf/8e/17/g0/NE_Metalle.pdf. Accessed 22 Jul 2022
 34. METALCOR GmbH, “Datenblatt-Hafnium”. <https://www.metalcor.de/wp-content/uploads/2013/04/Datenblatt-Hafnium.pdf>. Accessed 22 Jul 2022
 35. von Goldbeck OK (1982) *IRON—binary phase diagrams*. Springer, Berlin Heidelberg, Berlin, Heidelberg
 36. ASM International (1992) *Alloy phase diagrams*, 10th edn. ASM International, Materials Park, Ohio

Publisher's note Springer Nature remains neutral with regard to jurisdictional claims in published maps and institutional affiliations.